6 Multiphase flow modelling

Most books on fluid mechanics, especially books on turbulence, will have a statement along the lines of 'most important fluid flows are turbulent'. That statement can be made for multiphase flows as well. Most of the flows around us are multiphase. They exist in nature, such as rain or snow in the sky, or the flow of a river, which may transport all kinds of solids and has a large interface with the air above it. Also, the flow of blood in our veins is a good example of a mixture of a fluid and particles. Such cases prevail even more so in industry, especially in the processing industry. In the pharmaceutical industry, pills are made from small particles. Also droplets can be dispersed so that they can be inhaled into lungs. There is an abundance of multiphase flows in chemical-process industries, e.g. flow of catalyst particles, fuel, plastics, gases, etc. The energy-producing industry has many examples too, such as the burning of coal particles and fuel sprays and the boiling of water. Bubbly flows prevail in the nuclear industry, where the science of studying multiphase flows all started. These are just a few of the multitude of examples of multiphase flows. Some examples of multiphase flows and their applications are shown in Table 6.1.

The word 'phase' in multiphase flows refers to the solid, liquid or vapour state of matter. The prefix 'multi' means multiple. So a multiphase flow is the flow of a mixture of phases such as gases (bubbles) in a liquid, or liquid (droplets) in gases or particles in liquids and/or gases. This definition should not be taken too strictly; for instance, the flow of two immiscible liquids does not contain multiple phases in a thermodynamic sense, yet, because there are multiple different liquids, and this is in fact quite similar to the situation of a droplet in a gas flow, they are still considered within the research area of multiphase flow. A more detailed disussion of multiphase flows can be found in [16].

The research area of multiphase flows is extremely broad and not very well defined. This has led to a very wide field of research, both fundamental and applied. It has also led to a lot of confusion – so much confusion that, today, there is not even agreement upon the governing equations which are to be used, let alone all the empirical closure models obtained from measured data. There are some areas where reliable ab-initio simulations are possible, whereas in other areas only parameter studies around experimentally validated simulations are possible. In general simulations of multiphase flows are reliable at low particle loading with particles that follow the continous phase closely. In contrast, multiphase systems that are dominated by non-ideal particle–particle collisions are very difficult so simulate accurately. This chapter tries to give an overview of the modelling

Table 6.1 Summary of two-phase flow systems and some industrial applications

Continuous phase–dispersed phase	Industrial applications
Gas–solid flows	Pneumatic conveying, fluidized beds, solid separation (filters, cyclones)
Liquid–solid flows	Stirred vessels, liquid–solid separation, hydraulic conveying
Gas–liquid (droplet) flows	Spray drying, spray cooling, spray painting
Liquid–droplet flows	Mixing, separations, extraction
Liquid–gas (bubble) flows	Flotation, aeration, bubble columns

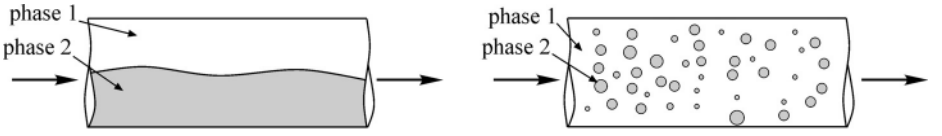

Figure 6.1 A separated (stratified) multiphase flow (left) versus a dispersed multiphase flow (right).

possibilities for dispersed and separated two-phase flows. Bubble and drop break-up and coalescence and population-balance modelling are not included.

6.1 Introduction

An important classification of multiphase flow is made in terms of whether the different phases present in the flow are separated or dispersed, as shown in Figure 6.1. In a dispersed flow, one phase is typically present in the form of particles or droplets and there are many individual interfaces. In a separated flow, the phases present are relatively separated, with only a few interfaces.

Commonly, dispersed two-phase flows are separated into two types of flow regime, the dilute regime and the dense regime. In the dilute regime, the spacing between the particles or droplets is quite large, so their behaviour is governed by the continuous phase (fluid) forces. In dense phase systems, the spacing is smaller, so the inter-particle interactions are typically very important. Very roughly, flows with a spacing of less than ten particle diameters are considered to be dense.

6.1.1 Characterization of multiphase flows

Several, mostly dimensionless, parameters are used to characterize multiphase flows. The most important one is the volume fraction, which defines how much of the local volume is occupied by either of the phases. The dispersed-phase volume fraction is the volume occupied by the particles in a unit volume,

$$\alpha_{\mathrm{d}} = \frac{\sum_{i=1}^{N_{\mathrm{d}}} V^i}{V}, \tag{6.1}$$

where V^i is the volume occupied by particle or droplet i and N_d is the total amount of particles or droplets present in volume V. The characteristic size of the dispersed phase is given as

$$D_{\mathrm{d},i} = \frac{6(V^i)}{\pi}^{1/3}, \tag{6.2}$$

which assumes that the volume occupied by one particle has a spherical shape. For some types of particle this is not a very good approximation, for instance for a fiber or a deformed droplet. Then, a sphericity factor depending upon the area or volume of the particle as seen by the flow can be introduced.

The 'typical' distance between the particles, assuming that they are homogeneously arranged, is given by

$$L = D_\mathrm{d}\left(\frac{\pi}{6\alpha_\mathrm{d}}\right)^{1/3}, \tag{6.3}$$

and this is one of the parameters used to determine the importance of inter-particle interactions. The volume fraction of the continuous phase is given as

$$\alpha_\mathrm{f} = 1 - \alpha_\mathrm{d}. \tag{6.4}$$

Typically, the inertia of the phases in multiphase flow modelling is expressed in terms of the bulk density, $\alpha_\mathrm{d}\rho_\mathrm{d}$, instead of just the intrinsic density ρ_d. The bulk density is a measure for the potential inertia, and will thus be employed to construct the mass and momentum balances. The mixture density is the sum of the dispersed-phase density and the continuous-phase density.

Sometimes, in the engineering literature, the flux of the dispersed phase is expressed in terms of the mass loading, which is defined as the mass flux of the dispersed phase divided by that of the continuous phase,

$$m = \frac{\alpha_\mathrm{d}\rho_\mathrm{d}U_\mathrm{d}}{(1-\alpha_\mathrm{d})\rho_\mathrm{f}U_\mathrm{f}}. \tag{6.5}$$

Timescales and length scales are important measures in fluid mechanics and even more so in the case of the timescale for a particular physical mechanism in the multiphase flow. Examples of these mechanisms are collisions, inertia and dissipation.

It is difficult to define one unique scale for a flow or a dispersed phase, since these are given by large distributions. But it is still useful to determine or estimate a dominant dimensionless number specifying the ratio of a dispersed-phase timescale and a continuous-phase timescale. This ratio is called the Stokes number, and a Stokes number much bigger than unity means the particles are relatively insensitive to that specific timescale of the continuous-phase behaviour. For instance, the turbulence Stokes number is given as

$$St_\mathrm{T} = \frac{\tau_\mathrm{d}}{\tau_\mathrm{T}}, \tag{6.6}$$

where τ_d is the timescale of the dispersed phase and τ_T is the relevant timescale of the turbulence. An estimation of the particle response time is obtained by solving Eq. (6.9)

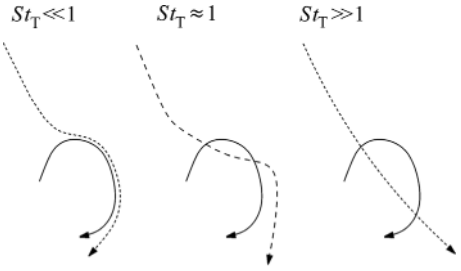

Figure 6.2 Effects of a turbulent eddy (solid line) on particle trajectory (dashed line) for different Stokes-number limits.

below. For simple flow at low Reynolds numbers the response time will be

$$\tau_d = \frac{\rho_d D^2}{18\mu_f}. \tag{6.7}$$

When $St_T \to 0$, for instance for very small particles, the particles follow the flow completely. For flows in which $St_T \to \infty$, the behaviour of the particles is uncorrelated with the flow characteristics. This effect is depicted in Figure 6.2.

Another important Stokes number is the collision Stokes number,

$$St_c = \frac{\tau_d}{\tau_c}, \tag{6.8}$$

where τ_c represents the timescale of the inter-particle interactions. If $St_c < 1$, a flow may be assumed dilute; if $St_c > 1$, a flow may be considered dense. This measure can be used as an additional measure to determine the importance of particle–particle interactions, next to that of particle spacing.

6.1.2 Coupling between a continuous phase and a dispersed phase

A general classification of dispersed two-phase flows with regard to the interaction with the continuous phase was provided by Elgobashi in 1994. There are three possible ways of coupling, which are listed in Table 6.2. If the particles do not influence the flow and their interactions are negligible, only the effect of the fluid on the particles is important. The terms describing how the particles affect the flow and how they affect each other may be neglected. This is defined as one-way coupling.

If particles have a Stokes number larger than unity or the volume fraction is sufficiently large to affect the average denisty of the mixture, their effect on the flow is no longer negligible, and modelling of the effect of the particles on the flow has to be incorporated into the governing equations for the continuous phase. If the flow is still sufficiently dilute, inter-particle interactions may safely be neglected. This is defined as two-way coupling.

If the volume fraction of the dispersed phase is sufficiently large, typically above 10^{-3}, inter-particle interactions become important. Inter-particle interactions may be collisions, but also more indirect phenomena, such as two particles approaching each

Table 6.2 The various types of coupling between the dispersed phase and the continuous phase. The choice of coupling can be made on the basis of the length scale of the dispersed phase, or on the basis of the Stokes number

Type of coupling	Definition	Implementation
One-way	Dispersed phase senses continuous phase, but the continuous phase is unaffected	Particle tracking may be done in a post-processor
Two-way	Dispersed phase senses continuous phase and continuous phase senses dispersed phase	The presence of the dispersed phase should be reflected in the governing equations of the fluid
Four-way	Dispersed particles interact	A model for particle–particle interactions should be included

other in a viscous liquid. Although they will most probably not collide, their interaction may still be important. This is defined as four-way coupling (note that one particle affecting the other and the other affecting the first is counted as two coupling terms).

Note that this classification does not specify how accurate a model should be. The dispersed phase may be represented by a momentum source in the governing equations for the continuous phase, or, alternatively, the complete flow around a particle may be resolved. Although they are very different in terms of the level of detail, both these models fall into the category of two-way coupling.

6.2 Forces on dispersed particles

Newton's second law can be applied to the dispersed particles. The main controversy has been over how to describe the forces acting on the particles. The original work by Basset (1888), Boussinesq (1885) and Oseen (1927), abbreviated as the BBO equation, described a few small particles in a uniform flow with particle Reynolds number $Re_\mathrm{P} \ll 1$. The original work was later adjusted for higher particle Reynolds numbers and turbulent flows. In a more general framework, the forces on a single particle are given by

$$m_\mathrm{d}\frac{\mathrm{d}U_{i,\mathrm{d}}}{\mathrm{d}t} = F_{i,\mathrm{Drag}} + F_{i,\mathrm{Press}} + F_{i,\mathrm{Virt}} + F_{i,\mathrm{History}} + F_{i,\mathrm{Bouy}} + F_{i,\mathrm{Lift}} + F_{i,\mathrm{Therm}} + F_{i,\mathrm{Turb}} + F_{i,\mathrm{Brown}}, \tag{6.9}$$

where $U_{i,\mathrm{d}}$ is the linear velocity of the particle, m_d is the mass of the particle, $F_{i,\mathrm{Drag}}$ is the drag force, $F_{i,\mathrm{Press}}$ is the pressure force due to the pressure gradient, $F_{i,\mathrm{Virt}}$ is the virtual mass force due to acceleration of the surrounding fluid, $F_{i,\mathrm{History}}$ is the history or Basset force due to changes in the boundary layer, $F_{i,\mathrm{Bouy}}$ denotes forces due to gravity, $F_{i,\mathrm{Lift}}$ is the Saffman and Magnus lift force due to the velocity gradient and particle rotation, $F_{i,\mathrm{Therm}}$ is the thermophoretic force due to a temperature gradient, $F_{i,\mathrm{Turb}}$ denotes forces due to turbulent fluctuations and $F_{i,\mathrm{Brown}}$ is the Brownian force due to molecular collisions. These forces are described briefly below and a more detailed discussion can be found in [17].

The Magnus force is due to the rotation of the particle and a torque balance is required. This balance between rotational velocity, ω_i, inertia, I_i, and torque, T_i, is given by

$$I_i \frac{\mathrm{d}\omega_i}{\mathrm{d}t} = T_i .$$

However, the Magnus force is usually small and not well defined outside the laminar region, and the torque balance is not discussed further in this book.

The forces in Eq. (6.9) above are briefly described below. Note that the detailed flow around the particles is not resolved. The model requires that the particles are much smaller than the computational cell and that the continuous phase is resolved on a large scale. The effect of the dispersed phase on the continuous phase is treated as a source term arriving from all particles in the cell.

For a single particle the *drag force* is expressed as a function of the relative velocity between the two phases,

$$F_{i,\mathrm{Drag}} = \frac{1}{2} A_\mathrm{d} C_\mathrm{D} \rho_\mathrm{f} \left| U_\mathrm{f} - U_\mathrm{d} \right| \left(U_{i,\mathrm{f}} - U_{i,\mathrm{d}} \right), \tag{6.10}$$

where A_d is the projected area normal to the flow, i.e. $\pi D_\mathrm{p}^2/4$ for a sphere. The drag coefficient C_D is discussed in more detail in Section 6.4.1.

The second term represents the *pressure and shear forces* from the fluid on the particle. This is usually expressed in terms of the pressure and shear gradient over the particle surface. Assuming a constant pressure and shear gradient over the volume of the particle, this force can be written

$$F_{i,\mathrm{Press}} = V_\mathrm{d} \left(-\frac{\partial P}{\partial x_i} + \frac{\partial \tau_{ij}}{\partial x_j} \right), \tag{6.11}$$

where V_d is the volume of the particle.

The third term represents the *virtual-*, *apparent-* or *added-mass force*. This force arises from the acceleration or deceleration of the fluid surrounding an accelerating or decelerating particle. The effect of this term is an increase in the apparent mass of the particle, whence the name added-mass force. This force is written in the form

$$F_{i,\mathrm{Virt}} = -C_\mathrm{VM} \rho_\mathrm{f} V_\mathrm{d} \frac{\mathrm{D}}{\mathrm{D}t} (U_{i,\mathrm{d}} - U_{i,\mathrm{f}}), \tag{6.12}$$

where $\mathrm{D}/\mathrm{D}t$ is the substantial operator and represents the relative acceleration of the particle compared with the fluid along the path of the particle. The virtual-mass force coefficient C_VM is usually close to 0.5, which indicates that a volume of the continuous phase corresponding to half the volume of the particle is accelerated with the particle. This force can be neglected when the density of the continuous phase is much lower than the density of the particle and the virtual mass is much less than the mass of the particle.

The fourth term, the *history force*, arises from the time required to develop the boundary layer around the particle when the particle is accelerated or decelerated. This development leads to a separation of timescales between the fluid and the particle, thereby creating the necessity for the time integral in the force. This time integral makes

the history force computationally very expensive – the calculation times may increase by an order of magnitude.

The fifth term represents the *bouyancy force*, the volume of the particle multiplied by the density difference between the phases and the gravitational acceleration constant.

The *Saffman and Magnus lift forces* are due to the higher velocity on one side of the particle arising from flow in a velocity gradient (the Saffman lift force) or rotation of the particle (the Magnus lift force). Accurate models are available only for spherical bodies at low particle Reynolds numbers. There is very little empirical data for both types of lift force at higher Reynolds numbers. Owing to boundary-layer separation and deformation of fluid particles, even the direction of the lift force can be difficult to predict.

The *thermophoretic force* represents the force due to a temperature gradient in the fluid. Hot molecules move faster than cold molecules and a large temperature gradient will give a net force in the direction opposite to the temperature gradient. This thermophoretic force is important only for very small particles, and will lead to a separation of particles depending on their size.

The origin of the *Brownian force* is random collisions of individual molecules. This force is usually modelled as Gaussian white noise. The momentum transferred by collision of individual molecules is very small and the Brownian force is important only for submicrometer particles.

The *forces due to turbulence* are often modelled as a random addition to the fluid velocity that is sustained for a time corresponding to the minimum of the lifetime of the turbulent eddies and the time taken for a particle to pass through a turbulent eddy.

The importance of the terms in the above equation of motion for one particle can be analysed by dividing all the forces by the particle density. If the particle density is much larger than the fluid density, as in gas–solid and gas–droplet flows, terms linear in ρ_f/ρ_d may be neglected. This means that only drag, the pressure and shear-stress gradient, and the buoyancy are important in such flows. If terms containing ρ_f/ρ_d may not be neglected, such as for rising bubbles and liquid–solid flows, the added-mass force and the history force are typically important. It is much more difficult to calculate the trajectories of particles in such flows.

The original BBO equation is valid for one (or very few) particles in a homogeneous flow with particle $Re < 1$. Most industrial applications do not deal with a few particles in a homogeneous and low-Reynolds-number flow, so empirical extensions of the forces from their original derivation are required. For the drag force, this has been a very successful approach; here the empirical coefficient is called the drag coefficient. The lift coefficient, virtual-mass coefficient, and history-force coefficient have been found to be more prone to error, and the form of the terms in Eq. (6.9) may be less suitable. Closure models for these terms are discussed later.

6.3 Computational models

There are many different kinds of model available for multiphase flow. The models presented in this book can be subdivided into five main classes:

- the Euler–Lagrange model
- the Euler–Euler model
- the mixture or algebraic-slip model
- the volume-of-fluid (VOF) model
- porous-bed models.

In *Euler–Lagrange modelling* the fluid phase is modelled as a continuum by solving the Navier–Stokes equations, while for the dispersed phase a large number of individual particles is modelled. The dispersed phase can exchange momentum, mass and energy with the fluid phase. Since the particle or droplet trajectories are computed for each particle or for a bundle of particles that are assumed to follow the same trajectory, the approach is limited to systems with a low volume fraction of dispersed phase.

In *Euler–Euler models* the different phases are all treated as continuous phases, and momentum and continuity equations are solved for each phase. The Euler–Euler model can handle very complex flows, but does not always give the best results since empirical information is needed in order to close the momentum equations. Typical applications are risers and fluidized beds.

In the *mixture model* (algebraic-slip model) the flows of phases are assumed to interact strongly and it is not necessary to solve the momentum balances for the different phases separately. In this model the viscosity is estimated for the mixture. The velocities of the different phases are thereafter calculated from buoyancy, drag and other forces, giving the relative velocities in comparison with the mean velocity of the mixture. Typical applications are bubble columns, fine particle suspensions and stirred-tank reactors.

The *volume-of-fluid (VOF) model* is an Euler–Euler model whereby the interface between the different phases is tracked. The model is suitable for stratified flow, free surface flows and movement of large bubbles in liquids. Since the interface between the fluids must be resolved, it is not applicable for a system with many small drops or bubbles.

In the *porous-bed model*, the pressure drop across a porous bed is modelled. In a bed containing many particles, it is not possible to resolve the geometry and solve the Navier–Stokes equations. Instead the pressure drop is calculated from an equation similar to the Ergun equation for the pressure drop in fixed beds [18].

6.3.1 Choosing a multiphase model

In selecting the most appropriate multiphase model, the physics of the system must be analysed and understood. Initially, there are some questions that must be asked.

- Are the phases separated or dispersed?
- Will the particles follow the continuous phase? What is the Stokes number?
- How large are the local volume fractions?
- How many particles are there in the system?
- What kind of coupling occurs? Is it one-, two- or four-way coupling?

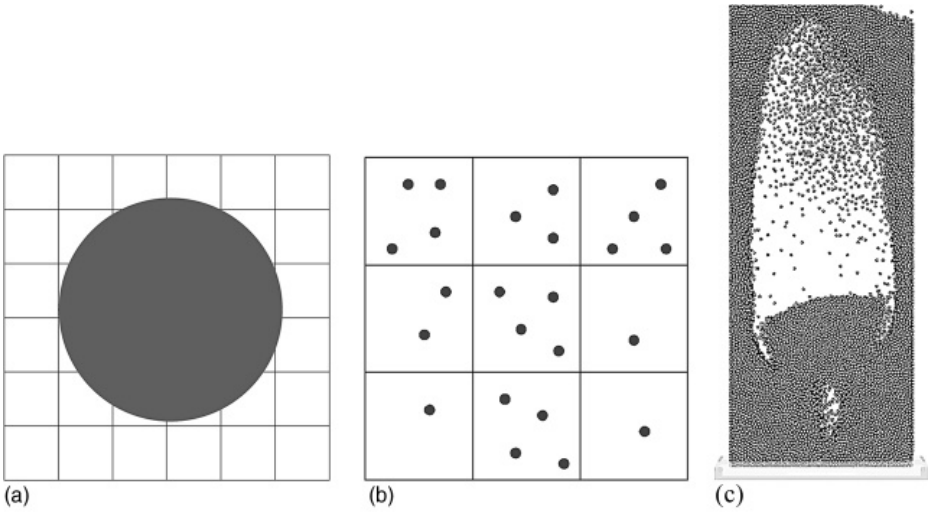

Figure 6.3 The concept of true direct numerical simulation (a), and the point-particle approach (b). In (c) an example of the point-particle approach is shown.

For separated flows only the VOF model will work. The model predicts the location of the interface and uses single-phase models to predict the flow in each phase. The model requires a fine mesh to resolve the curvature of the interface.

The porous-bed model is applicable to a system dominated by viscous and inertial forces, and the pressure drop can be calculated as a function of the flow properties by using an empirical a-priori given function.

For dispersed multiphase systems several models are possible. The most accurate is usually the Euler–Lagrange model. It works well for systems with one- or two-way coupling, but requires additional closures for four-way coupling. In such cases the computational time increases and the quality of the simulations is poor except for very ideal systems. The limitation for the Euler–Lagrange model is the number of particles. A few hundred thousand particles or bundles of particles is the limit on a desktop computer.

The general models for dispersed multiphase flow are the mixture and Euler–Euler models. The mixture model requires that the Stokes number is low and that the phases accelerate together. The mixture model is more stable and faster than the Euler–Euler model and should be used whenever possible. It may also be used to obtain good initial conditions for an Euler–Euler simulation. The Euler–Euler approach can be used when no other model is possible.

6.3.2 Direct numerical simulations

Resolving the behaviour of a flow all the way down to the smallest scales is called direct numerical simulation (DNS). If particles have a fluid Stokes number larger than unity, hence two-way coupling, the flow around the particles must be resolved as shown in Figure 6.3(a). Although this is possible, it requires efficiently developed algorithms and

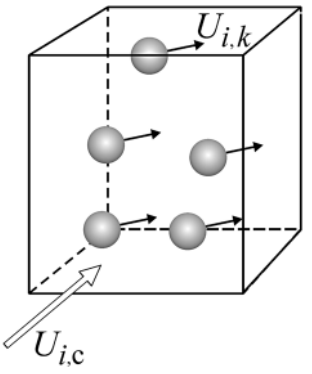

Figure 6.4 Lagrangian control volume.

a lot of patience; at the time of writing, only about 10^3 particles can be considered. This might be useful for research objectives, but is useless for industrial purposes.

6.3.3 Lagrangian particle simulations, the point-particle approach

In this technique the particles are tracked individually, and the gas phase is treated in a continuous framework. This can be done by resolving the flow around the particles, or by representing the particles as source terms in the flow. This is depicted in Figures 6.3(a) and (b), and in Figure 6.3(c) a Lagrangian particle simulation for a small fluidized bed is shown.

In point-particle-approach simulations, the single-phase Navier–Stokes equations for the continous phase are solved in conjunction with tracking the individual particles,

$$\frac{\partial(\alpha_\mathrm{f}\rho_\mathrm{f})}{\partial t} + \frac{\partial(\alpha_\mathrm{f}\rho_\mathrm{f}U_{i,\mathrm{f}})}{\partial x_i} = S_\mathrm{C}, \tag{6.13}$$

$$\frac{\partial(\alpha_\mathrm{f}\rho_\mathrm{f}U_{i,\mathrm{f}})}{\partial t} + U_{i,\mathrm{f}}\frac{\partial(\alpha_\mathrm{f}\rho_\mathrm{f}U_{j,\mathrm{f}})}{\partial x_i} = -\alpha_\mathrm{f}\frac{\partial P}{\partial x_i} + \frac{\partial(\alpha_\mathrm{f}\tau_{ij,\mathrm{f}})}{\partial x_j} + S_{i,\mathrm{p}}, \tag{6.14}$$

where S_C is a source term describing mass transfer between the phases and $S_{i,\mathrm{p}}$ represents momentum exchange between the particles and the fluid. All forces on the right-hand side of Eq. (6.9) except gravity are due to interaction with the continous phase and must appear in the source term $S_{i,\mathrm{p}}$ of Eq. (6.14). Equation (6.14) is written per volume and Eq. (6.9) per particle, and the term $S_{i,\mathrm{p}}$ must include the number of particles, per volume, i.e. $n/V = 6\alpha_\mathrm{d}/(\pi D_\mathrm{p}^3)$ assuming spherical particles. For successful employment of the Euler–Lagrange model, the particles have to be much smaller than the fluid-phase grid cells as shown in Figure 6.4. This restriction arises because the velocity field, U_f, required to calculate the source term needs to be the undisturbed velocity field.

The flow of the continuous fluid (Eqs. (6.13) and (6.14)) can be solved with traditional RANS or LES models with the additional terms describing the interaction between the continuous and dispersed phases. The movement of all the particles is simulated by

integrating the trajectory Eq. (6.15) and the force balance Eq. (6.9) with given initial position for all particles:

$$\frac{\mathrm{d}x_i}{\mathrm{d}t} = U_{i,\mathrm{d}}. \tag{6.15}$$

The number of particles is limited because it involves solving an ODE for all particles. However, it is possible to bundle particles that behave identically into packages containing thousands of particles. This will give a correct source term for the continuous phase. The limitation is that the bundle will be modelled assuming that the properties at the centre of gravity for the bundle are valid for all particles and that the source term for the bundle is at the centre of gravity.

Euler–Lagrange models are usually accurate at low volume fraction with one- or two-way coupling. At higher volume fraction, when the particles collide the model requires additional closures (see Section 6.4.2). The simulations become very demanding at high particle loading due to the high number of collisions. It is not possible to calculate all potential collisions beween all particles, and most CFD programs simulate collisions only for particles that are within the same computational cell. More advanced algorithms may also include neighbouring cells. In all cases, the number of particles must be low and the time step must be limited so that no particle moves by more than one computational cell in one time step. In addition it is not possible to model how the particles will collide. Even if the momentum is conserved and the absolute value of the velocity is known, the direction is unknown. There are stochastic models that calculate a probability distribution of velocities of a large number of collisions after each time step. However, the use of Euler–Lagrange models with four-way coupling is not yet a feasible approach in engineering.

Turbulence modelling

The continuous phase may be modelled using standard RANS or LES methods. In the k–ε model a source term for the additional turbulence energy arising from the movement of the particles may be included. The turbulence energy generated from the movement of particles can be formulated as a source term in the equation for k:

$$S_k = \frac{\alpha_\mathrm{d}\rho_\mathrm{d}}{\tau_\mathrm{d}\rho_\mathrm{c}} \left(U_\mathrm{d} - \langle U_\mathrm{f}\rangle\right)^2. \tag{6.16}$$

The dissipation is assumed to increase in proportion to the increase in kinetic energy divided by the timescale for the large eddies, k/ε, as in the standard ε equation

$$S_\varepsilon = C_{\varepsilon 3}\frac{\varepsilon}{k}S_k, \tag{6.17}$$

where the constant $C_{\varepsilon 3}$ is about 1.8. However, the size of the turbulent eddies formed by the particles is usually much smaller than that of the energy-containing eddies that contain most of the turbulent kinetic energy and also transport most of the momentum. The small eddies formed by the particles will decay very fast and transport only a small fraction of the momentum. The extra source term should be included only when the turbulent eddies formed by the particles are large compared with the energy-containing eddies.

The effect of fluid-phase turbulence on the particles may be important, depending upon the Stokes number. In determining a drag force, the instantaneous drag forces on each particle are averaged into a drag force, which becomes a function of the mean or average relative velocity. The turbulent eddies in the continous phase will move the single particles in all directions and away from the average path. At the end particles injected at the same point will not end up at the same position due to the turbulence, and this phenomenon must be taken into account.

The information on the turbulence provided by RANS models is available only in statistical terms, for instance, in terms of the turbulent kinetic energy and energy-dissipation rates. To couple the behaviour of the particles effectively with the local fluid properties, however, instantaneous fluid properties are required. A popular way of determining a non-unique set of instantaneous fluid properties from the given statistical turbulence models is use of the so-called random-walk models. The instantaneous fluid velocity at a particle location is determined from the averaged fluid velocity, which is deterministic, and a random component for which the magnitude, direction and timescales obey the statistical (averaged) properties of the local fluid turbulence.

In the discrete-random-walk (DRW) model it is assumed that the effect of turbulence can be modelled by adding a random velocity to the continuous phase for a specific time T, where T is the time the particle spent in a turbulent eddy. This time is estimated as the minimum of the time taken for a particle to pass through the turbulent eddy and the lifetime of the turbulent eddy. The time taken to pass through the turbulent eddy is estimated from the size of the turbulent eddy and the slip velocity,

$$T \approx -\tau \ln\left(1 - \frac{l}{\tau |U_\mathrm{d} - \langle U_\mathrm{f}\rangle|}\right), \tag{6.18}$$

where τ is the particle response time (Eq. (6.7)) and l is the size of the turbulent eddy (Eq. (4.19)). The lifetime of a turbulent eddy in RANS models is

$$T \propto \frac{k}{\varepsilon}. \tag{6.19}$$

The turbulent velocity fluctuations are assumed to have a Gaussian probability distribution and the turbulent fluctuations are added to the continuous-phase velocity

$$u_i' = \xi_i \sqrt{u_i^2}, \tag{6.20}$$

where ξ_i is a Gaussian random number.

In isotropic turbulence $\langle u_1^2\rangle = \langle u_2^2\rangle = \langle u_3^2\rangle = 2k/3$ and the continuous-phase velocity fluctuation is calculated from

$$u_i = \xi_i \sqrt{\frac{2k}{3}}. \tag{6.21}$$

All three velocity fluctuations are known in Reynolds stress modelling and all the individual fluctuating components can be calculated. The random velocity u_i' is then added to the average fluid velocity $\langle U_{i,\mathrm{f}}\rangle$ and kept constant during the time step defined by T above. A new random number ξ_i is chosen after each time step.

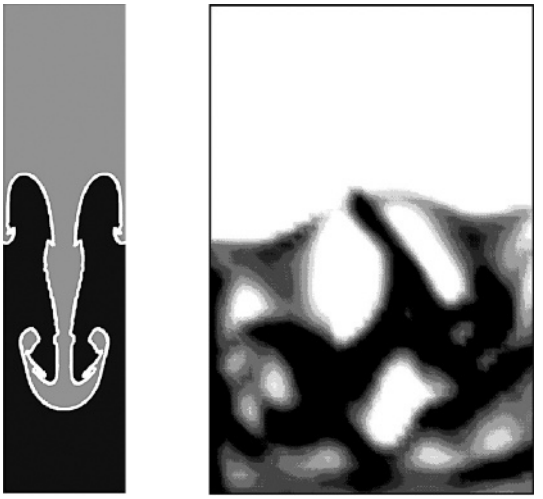

Figure 6.5 A stratified flow simulation (left) versus a dispersed flow simulation (right).

6.3.4 Euler–Euler models

The Euler–Euler model treats a dispersed multiphase flow as two (or more) fully interpenetrating quasi-fluids, and is therefore often referred to as the two-fluid model. The two-fluid model is derived by ensemble averaging or volume averaging. A very important quantity appearing in the equation because of the averaging is the volume fraction α_k. This quantity alone does not say anything about the size or behaviour of the dispersed phase, and this generally comes in via closure models. Within the Euler–Euler framework both stratified and dispersed flow are modelled. In this book we present the Euler–Euler model as a general model for most kinds of multiphase flow, the mixture model as a simplification of the Euler–Euler model and the volume-of-fluid model for stratified flows as shown in Figure 6.5.

Intuitively, it is easiest to imagine the derivation of the two-fluid model in terms of volume averaging. A small volume, much smaller than that of the large-scale flow structures, but much larger than that of individual dispersed particles, in which both phases are present is used in this model. The volume fraction is defined on the basis of the distribution of phases and the size of the computational volume. The local instantaneous equations describing both phases may then be averaged in the volume, considering the bulk density of each of the phases. The two-fluid model equations for each phase are given by the following equations, where k is not an index but represents a phase:

$$\sum_k \alpha_k = 1, \tag{6.22}$$

$$\frac{\partial \alpha_k \rho_k}{\partial t} + \frac{\partial \alpha_k \rho_k U_{i,k}}{\partial x_i} = -\sum_{l=1}^{p} (\dot{m}_{kl} - \dot{m}_{lk}), \tag{6.23}$$

$$\frac{\partial \alpha_k \rho_k U_{i,k}}{\partial t} + \frac{\partial \alpha_k \rho_k U_{i,k} U_{j,k}}{\partial x_j} = -\alpha_k \frac{\partial P}{\partial x_i} + \frac{\partial \alpha_k \tau_{ij,k}}{\partial x_k} + \alpha_k \rho_k g_i + F_{i,k}, \tag{6.24}$$

where p represents the number of phases, $\dot{m}_{kl}$ mass transport from phase k to phase l and F_k the interaction force with the other phases. The difficulty of solving these sets of equations is twofold. First, these equations are difficult from a numerical point of view, since there are many coupled equations with one shared pressure. Secondly, to solve the equations, closure models are required for τ and F_k. Here τ represents the rheology of the phase, and very complex models are typically required if the phase is not a Newtonian fluid but, for instance, a particle mixture. Models for estimation of viscosity in multiphase flows are presented in Section 6.4.2. The interaction force with the other phases, F_k, typically comprises collisions with the other dispersed phases and all important physical mechanisms described by Eq. (6.9).

It is important to realize that all variables appearing in this equation are *averaged* variables, rather than real point variables. This makes concepts such as LES and RANS for the two-fluid model quite complex; the equation does not revert back to a DNS simulation on reducing the grid size.

All physical phenomena, apart from the quantities provided by the principle of momentum conservation, must be modelled by closure models. This includes the rheology of the dispersed phase and the momentum transfer between the phases. The continuous fluid is often modelled using a k–ε or RSM model, but the dispersed phases need more elaborate models. Some of these closure models are discussed later in this chapter.

Turbulence modelling

Standard k–ε and RSM models can be used with the Euler–Euler multiphase model for dilute systems and when the phases can be approximated with one set of momentum models for the mixture as in Section 6.3.2. For the continuous phase in a dilute system k is modelled with the standard k equation with an additional source term describing the additional turbulence energy arising from the relative velocities of the continuous phase and the dispersed phases. For the dispersed phases the timescales and length scales for the particles are used to evaluate dispersion coefficients and the turbulent kinetic energy for each phase.

For dense systems, when a turbulence model is required for each phase, the commercial CFD software usually includes only the k–ε model. These models tend to be very unstable, and the quality of the simulations is usually low. The simulations often need calibration and should be combined with validation experiments in similar systems.

6.3.5 The mixture model

The mixture model is similar to the Euler–Euler model, but assumes one more simplification. This simplification is that the coupling between the phases is very strong and the relative velocity between the phases is in local equilibrium, i.e. they should accelerate together. In performing a simulation with the mixture model, one set of equations is solved for the mixture, i.e. the unknowns are the flow properties of the mixture, not those of the individual phases. The flow properties of the individual phases can be reconstructed with an algebraic model for the relative velocity, which is often referred to as the algebraic-slip model. The individual phase's velocity relative to the mean velocity

is called the drift velocity and is denoted $U_{i,\mathrm{dr},k}$ for phase k, while the velocity relative to the continuous phase is the slip velocity. The advantage of employing the mixture model is that only one set of equations is computed, leading to a substantial decrease of computational effort compared with the full Euler model. This set of equations is given as

$$\frac{\partial \rho_\mathrm{m}}{\partial t} + \frac{\partial (\rho_\mathrm{m} U_{i,\mathrm{m}})}{\partial x_i} = 0, \tag{6.25}$$

$$\frac{\partial (\rho_\mathrm{m} U_{i,\mathrm{m}})}{\partial t} + \frac{\rho_\mathrm{m}\, \partial (U_{j,\mathrm{m}} U_{i,\mathrm{m}})}{\partial x_j} = -\frac{\partial P}{\partial x_i} + \frac{\partial \tau_{ij,\mathrm{m}}}{\partial x_j} + \rho_\mathrm{m} g_i - \frac{\partial \sum_k \alpha_k \rho_k U_{i,\mathrm{dr},k} U_{j,\mathrm{dr},k}}{\partial x_j}, \tag{6.26}$$

where the subscript m represents the mixture property and $U_{i,\mathrm{dr},k}$ the drift velocity for phase k, so that

$$U_{i,k} = U_{i,\mathrm{dr},k} + U_{i,\mathrm{m}}. \tag{6.27}$$

The last term in Eq. (6.26) arises from the nonlinear inertial term in the Navier–Stokes equations, which can be written as the second term on the left-hand side plus the last term on the right-hand side in Eq. (6.26), since

$$\frac{\partial \sum\limits_k \alpha_k \rho_k U_{i,k} U_{j,k}}{\partial x_j} = \frac{\rho_\mathrm{m}\, \partial (U_{i,\mathrm{m}} U_{j,\mathrm{m}})}{\partial x_j} + \frac{\partial \sum\limits_k \alpha_k \rho_k U_{i,\mathrm{dr},k} U_{j,\mathrm{dr},k}}{\partial x_j}. \tag{6.28}$$

The mixture properties are typically weighed by the volume fraction, e.g.

$$\mu_\mathrm{m} = \sum_\mathrm{m} \alpha_k \mu_k, \tag{6.29}$$

where the viscosity μ_k for dispersed flows may be estimated using the same models as in standard Euler–Euler modelling (see the discussion of granular flow models in Section 6.4.2).

Typically, a steady-state algebraic expression based on Eq. (6.9) is specified for the drift or slip velocity for each phase to close the mixture model. The volume fractions can be determined from the conservation equation for the continuity of each phase as described by Eq. (6.23).

Turbulence modelling

Standard RANS and LES models can be used for turbulence modelling using the average properties for density and viscosity. In the k–ε model the turbulent viscosity is calculated from k and ε in the same way as for single-phase flow with a small correction for systems in which the drift velocity is large compared with the velocity of the turbulent eddies. The effect of turbulent diffusion is also added to the drift velocity calculated using Eq. (6.9),

$$(U_{i,\mathrm{dr},k})_\mathrm{turb} = U_{i,\mathrm{dr},k} - \frac{\mu_\mathrm{t}}{\sigma_\mathrm{t}} \left(\frac{1}{\alpha_k} \frac{\partial \alpha_k}{\partial x_i} - \frac{\partial \alpha_\mathrm{f}}{\partial x_i} \right), \tag{6.30}$$

where the turbulence Schmidt number, σ_t, is of the order of 0.7.

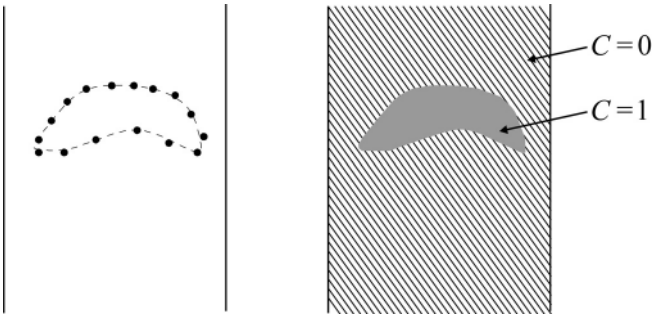

Figure 6.6 A rising bubble from the perspective of the level-set method (left) and the volume-of-fluid method (right).

6.3.6 Models for stratified fluid–fluid flows

One objective in modelling stratified fluid flows is to track the interface, and the Lagrange and Euler–Euler models are not suitable for modelling stratified flows. Instead, front-tracking, level-set or volume-of-fluid methods should be employed, as shown in Figure 6.6. These models may also be employed for DNS of dispersed multiphase flows in cases with a few deformable interfaces, for instance to study the deformation of two colliding droplets. Note that all of these methods assume a no-slip condition at the fluid–fluid interface, and thus have to be resolved to the Kolmogorov length scale. The methods are combined with a single-phase Navier–Stokes type equation,

$$\frac{\partial U_i}{\partial t} + \frac{\partial (U_i U_j)}{\partial x_j} = -\frac{1}{\rho_\mathrm{f}} \frac{\partial P}{\partial x_i} + \frac{1}{\rho_\mathrm{f}} \frac{\partial \tau_{ji}}{\partial x_j} + g_i, \tag{6.31}$$

where the local fluid properties, e.g. density and viscosity, are given by the presence of the phase,

$$\phi_\mathrm{f}(x) = \sum \alpha_k \phi_{\mathrm{f}k}. \tag{6.32}$$

If only one phase is present the properties will be for that phase, and a volume-weighted average is used for cells that are shared between two or more phases. The volume fraction is modelled with the continuity equation (6.23). In addition, an extra source term to account for surface-tension effects is also required in these cells.

Although front-tracking, level-set and volume-of-fluid methods are similar, there are some distinct differences, leading to the applicability of each method for different problems. However, only volume-of-fluid methods will be described here.

Volume-of-fluid methods

Volume-of-fluid (VOF) methods use the value of the volume fraction on a grid-cell basis to describe the position of the interface. The advective part of the equation is solved by special advection schemes, such as Lagrangian schemes, geometrical schemes and compressive schemes. These schemes can deal much better with cross-flow situations, and tend to be more mass-conserving than their level-set counterparts. Strictly speaking,

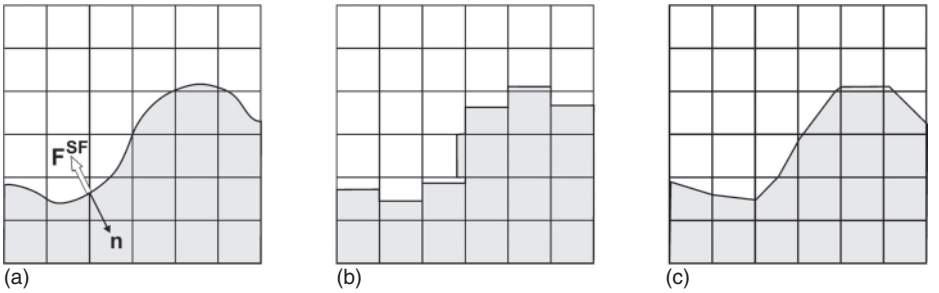

Figure 6.7 Volume-of-fluid (VOF) modelling of a fluid–fluid surface: (a) is the real surface, (b) the volume fraction calculated by the VOF model and (c) the linear reconstruction of the surface.

however, the accuracy is still of first order and a very fine mesh is needed. Typically, about 20 cells/diameter will be needed in order to obtain satisfactory resolution of a spherical bubble or drop.

As soon as an interface between two different fluids ceases to be straight, it has a finite curvature and surface-tension forces may become important. Usually, the surface-tension force is included as an additional momentum source term in a stratified flow model:

$$\frac{\partial(\rho U_i)}{\partial t} + U_i \frac{\partial(\rho U_i)}{\partial x_i} = -\frac{\partial \tau_{ij}}{\partial x_j} + \frac{\partial P}{\partial x_i} + \rho g_i + S_{i,\mathrm{s}}. \tag{6.33}$$

It is only in the cells that are shared between the phases that the momentum equation is different from those in the single-phase models. A volume-weighted average of the physical properties according to Eq. (6.32) is used. Numerical instabilities may occur if the properties in the phases are very different, e.g. viscosity ratio $>10^3$.

The direction of the surface-tension force depends upon the interface normals, and its magnitude depends on the interface curvature as shown in Figure 6.7(a). The interface normal, n, in a continuous framework is mostly given as the gradient of the volume fraction,

$$n_i = \frac{\partial \alpha / \partial x_i}{\left| \sum_j \partial \alpha / \partial x_i \right|}. \tag{6.34}$$

To include surface tension between two immiscible, pure fluids in the framework of a front-tracking, VOF or level-set method, usually a continuum surface tension is applied in the form of

$$S_{i,\mathrm{s}} = \frac{\sigma \rho \kappa n_i \Gamma}{\frac{1}{2}(\rho_1 + \rho_2)}, \tag{6.35}$$

where σ is the surface-tension coefficient and is usually assumed to be constant, Γ is an interface indicator function and κ is the curvature of the interface. In the most popular continuum surface-tension model, that proposed by Brackbill *et al*. in 1992, the interface

indicator, the curvature of the interface and the interface normal are directly related to the volume fraction,

$$\Gamma = \left| \sum_j \frac{\partial \alpha}{\partial x_j} \right|, \tag{6.36}$$

$$\kappa = -\frac{\partial n_i}{\partial x_i}. \tag{6.37}$$

Hence, the curvature is a measure of how fast (magnitude) and in which direction (sign) the normal of an interface changes in space. The surface tension aims at minimizing the interface area. For bubbles or droplets, the minimized interface area is spherical; for a fully stratified flow, the minimized interface area is a straight line. The influence from surface tension can be neglected for capillary numbers $Ca = \mu U/\sigma \gg 1$ or Weber numbers $We = \rho L U^2/\sigma \gg 1$. For large interfaces, such as in stratified flows, but also for interfaces of bubbles or droplets of diameter larger then a few centimetres, the surface-tension force may be negligible. However, for very large curvatures, for example small bubbles with a diameter of a few millimetres, the surface tension may be dominant and in that case ensures that the interface is spherically shaped at all times.

One complication with surface tension not dealt with here is that, in mixtures and with temperature gradients, the surface tension is not constant, and there will appear tangential to the surface a force aiming at minimizing surface energy globally.

Turbulence modelling

In theory the interface should be resolved to the Kolmogorov length scale. This might not be possible in all cases, and standard RANS models must be used with caution. The bulk properties are used, and the damping of turbulence at the interface that is expected when the properties of the phases are very different might not be modelled corectly. Wall functions are not possible since the location of the interface is not given a priori. The k–ω model might be a better choice than the k–ε model, but will require a denser mesh. Large-eddy simulation works better with VOF since the momentum transport across the interface on the subgrid level is much less.

6.3.7 Models for flows in porous media

Flow in a porous medium is driven by the pressure drop over the medium. Examples of such flows occur in fixed-bed reactors, filters and trays in distillation columns. The pressure drop and the resistance of the medium are the most important terms in the governing equations for the fluid phase, i.e. the accelerations are usually small. It is generally not possible to resolve the flow around each object or cavity in a porous medium, so a rough estimate of the pressure drop over the bed is made. The pressure drop in a packed bed originates from viscous resistance, which is proportional to the

viscosity and velocity of the fluid phase, and an inertial resistance that is proportional to the density and the velocity squared,

$$\frac{\mathrm{d}P}{\mathrm{d}x_i} = -A\mu U_i - B\left(\frac{1}{2}\rho|U|U_i\right). \tag{6.38}$$

The simplest model for this is called Darcy's law, wherein inertial effects are neglected (i.e. $B = 0$). This is quite frequently used in, for example, simulations of the flow in oil reservoirs. A is then inversely proportional to the area of the pores in the reservoir.

The model of Ergun (dating from 1952) is valid for flow through packed beds for a wide range of velocities and includes both a viscous resistance and an inertial resistance,

$$A = \frac{150(1-\alpha)^2}{d_\mathrm{p}^2\alpha^3}, \tag{6.39}$$

$$B = \frac{1.75(1-\alpha)}{d_\mathrm{p}\alpha^3}, \tag{6.40}$$

where α is the void fraction and d_p is the particle diameter. Note that these values are valid only for flow though beds containing rigid spherical particles. For other types of particles, e.g. fibres and compressible particles, an empirical determination of A and B is required.

6.4 Closure models

Multiphase flow simulations without the requirement of closure models are either extremely computationally expensive, or apply only for very simplified situations. Almost all multiphase flow simulations for engineering applications need closure models to some extent. Most closure models are empirical, meaning that they are determined by experiments and are valid only for the conditions under which the experiments were performed. Some closure models are based upon more theoretical considerations, but most often require assumptions as well. It is important to verify these assumptions and determine whether they are applicable to the simulated conditions. Some of the most popular closure models are discussed here.

6.4.1 Interphase drag

Equation (6.10) is valid for a single particle, i.e. at low volume fraction of the dispersed phase. To model the drag between a fluid and dispersed particles at high volume fraction of the dispersed phase, the drag as formulated in Eq. (6.10) must be adjusted,

$$F_{i,\mathrm{D}} = \frac{1}{2}A_\mathrm{d}C_\mathrm{D}\rho_\mathrm{f}\alpha_\mathrm{f}^{-2.65}|U_{i,\mathrm{f}} - U_{i,\mathrm{d}}|\left(U_{i,\mathrm{f}} - U_{i,\mathrm{d}}\right), \tag{6.41}$$

where C_D represents the drag coefficient. For spherical particles, this coefficient is a scalar, since it does not depend upon the stream direction of the flow on the particle.

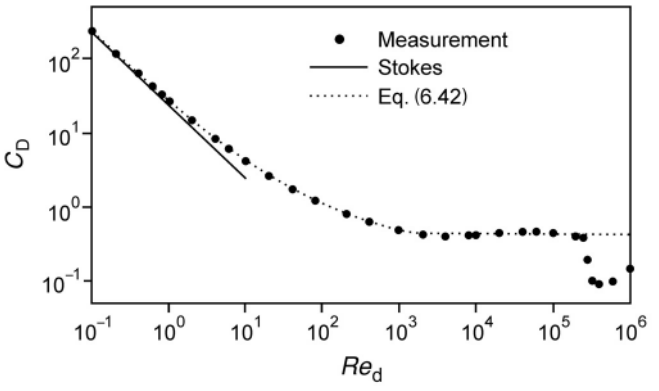

Figure 6.8 The standard drag curve for solid spheres in laminar flows.

Note that the drag is also dependent on particle loading as seen in the α_f dependence in Eq. (6.41). The drag coefficient has different Reynolds-number dependences in the viscous, intermediate and inertial flow regimes, as shown in Figure 6.8, and they are typically divided into three regions,

$$C_D = \begin{cases} \dfrac{24}{Re_d} & \text{if } Re_d < 0.5 \\ \dfrac{24}{Re_d}(1 + 0.15 Re_d^{0.687}) & \text{if } 0.5 < Re_d < 1000 \\ 0.44\alpha_f & \text{if } Re_d > 1000, \end{cases} \tag{6.42}$$

where the dispersed-phase Reynolds number, Re_d, is defined as

$$Re_d = \frac{\rho_f D_d |U_f - U_d|}{\mu_f}. \tag{6.43}$$

The drag coefficients in Eq. (6.42) are for particles in laminar continuous phase. The results from experimental studies of drag in turbulent flows have been contradictory, but usually the drag increases with increasing turbulence intensity.

The drag is in general lower for fluid particles, i.e. bubbles and drops due to the circulation of fluid within the particle. For fluid–fluid systems the drag will depend on the viscosity ratio $\kappa = \mu_d/\mu_c$ at low Reynolds numbers:

$$C_D = C_{D0}\left(\frac{\frac{2}{3} + \kappa}{1 + \kappa}\right), \tag{6.44}$$

where C_{D0} is the drag for a solid particle. For gases in pure liquids the drag is a function of Re for small bubbles and of the Eötvös number, $Eö$, for large bubbles,

$$C_D = \min\left(\frac{16}{Re}, \frac{8}{3}\frac{Eö}{Eö + 4}\right), \tag{6.45}$$

where the Eötvös number is defined as

$$Eö = \frac{g|\rho_p - \rho_c| D_p^2}{\sigma}. \tag{6.46}$$

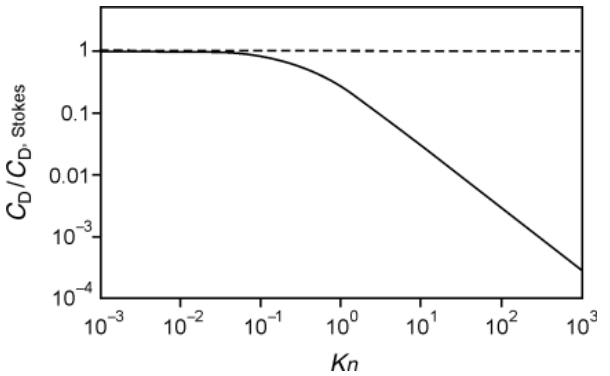

Figure 6.9 The rarefaction effect on drag.

For contaminated systems, e.g. tap water, the surface tension is not constant over the surface, making the bubble more rigid, and the drag coefficient is the same as for a solid particle, i.e. Eq. (6.42).

Much more complex equations are required for non-spherical particles. Large bubbles and drops are deformed and oscillate at high Reynolds number ($Re > 200$), and the drag coefficient cannot be described by a simple function.

In the models above, no slip is assumed for solid particles. In reality most gas molecules adsorb on the surface and will leave the surface in a random direction with the same temperature as the surface. A fraction of the molecules will bounce on the surface and transfer only a part of their momentum to the surface, and they will not be in thermal equilibrium with the surface. However, all molecules will soon collide with other gas-phase molecules, and these molecules will subsequently transfer their added momentum to the surface. The net effect is that the no-slip condition describes the momentum transfer accurately for large particles. However, for small particles or at low pressures the bouncing molecule may collide with other molecules far from the particle, and no secondary collision will occur. This is called the rarefaction effect and will be noticeable when the size of the particle is of the order of the distance between the molecules in the gas, i.e. the mean free path. This is described by the Knudsen number

$$Kn = \frac{\lambda}{d_p},$$

where λ is the mean free path and d_p the particle diameter. The mean free path is of the order of 75 nm in air at room temperature and 1 atm and rarefaction is important for particles with $d_p < 1$ μm. Figure 6.9 shows the correction of the standard drag curve due to rarefaction.

6.4.2 Particle interactions

In dense two-fluid flows, particle–particle interactions are important. The interactions can be indirect, whereby the dispersed particles never touch, or direct, whereby the

particles actually touch. Examples of indirect interactions occur in bubble columns, between interacting bubbles. However, indirect interactions between two particles may also occur; this is often referred to as the lubrication effect. When the fluid density and viscosity are low, interactions are most often direct.

Models for indirect interactions are required when the behaviour of continuous fluid between the two dispersed particles is not fully resolved. The models depend on how much of the fluid behaviour between the particles is unresolved, which may vary for each simulation. Typically, these models have the form of a long-range potential force, $1/r^{\gamma}$, where r is the distance between the bodies and γ provides a measure for the strength of the interaction. Such models are typically empirical.

Direct interactions typically involve solid particles colliding. There are two characteristic regimes for colliding particles, namely slow granular flow and rapid granular flow. Slow granular flow is characterized by very high volume fractions of solids, low relative velocities between the particles and enduring, multi-body contact. Rapid granular flow is characterized by moderate volume fractions of solids and binary, instantaneous collisions.

Lagrangian particle collisions

When dealing with particle–particle collisions, two types of collision model are widely employed, namely the hard-sphere model and the soft-sphere model. Hard-sphere models describe the dynamics of individual, binary collisions in terms of conservation of momentum and energy. In an ideal collision the momentum is conserved, and the momentum transferred during a collision can be quantified as

$$J = m_1(U_{\mathrm{d},1} - U'_{\mathrm{d},1}) = -m_2(U_{\mathrm{d},2} - U'_{\mathrm{d},2}), \tag{6.47}$$

where m_1 represents the mass of particle 1, $U_{\mathrm{d},1}$ the velocity prior to collision of particle 1 and $U'_{\mathrm{d},1}$ the velocity right after the collision. The post-collision velocities $U'_{\mathrm{d},1}$ and $U'_{\mathrm{d},2}$ can be found by making use of the principle of conservation of energy. More advanced hard-sphere models employ a coefficient of restitution, so part of the kinetic energy of the particles prior to collision is transferred to thermal energy during the collision.

The restitution coefficient describes the damping of velocity at the collision. It is defined as

$$e_{\mathrm{d}} = \frac{U'_{\mathrm{d},2} - U'_{\mathrm{d},1}}{U_{\mathrm{d},1} - U_{\mathrm{d},2}}. \tag{6.48}$$

A restitution coefficient of unity corresponds to ideal collision with no energy losses.

Soft-sphere models aim to estimate the local deformation of the particles during collision. This deformation is due to reversible deformation of the particle. The deformation is related to a linear ‘overlap’ of the particles during collision. The force resulting from the deformation is typically written in terms of a so-called spring–slider–dashpot model. The spring force is typically the dominant contribution, and is formulated as

$$F = -k\delta_n^{\alpha} n, \tag{6.49}$$

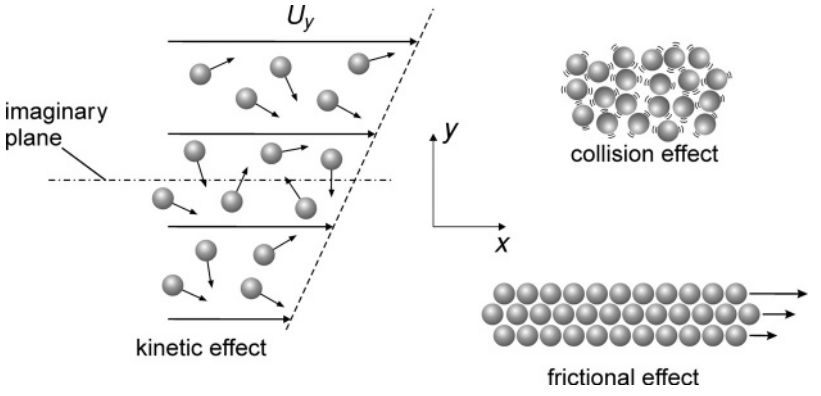

Figure 6.10 Mechanisms for momentum transfer beween particles.

where k is the spring constant, δ represents the overlap and the vector n represents the collision normal, the unit vector attaching the centres of the particles under collision. The exponent α equals 1 for simpler collision models, in which the spring constant cannot be directly related to the physical properties of the particles under collision, whereas a value for α of $3/2$ corresponds to a physically sounder model. The slider and dashpot components of the model represent the irreversibility of the collision, e.g. due to a coefficient of restitution, and the tangential interactions during a collision.

Granular flow models in the continuum framework

Viscosity models for the dispersed phase model the momentum transport between the dispersed particles within the same phase. The interactions with the other phases are described with the interaction coefficients. There are no particle–particle collisions at low loading with one- or two-way coupling, and the granular viscosity will consequently be negligible. The quality of viscosity models at high loading, i.e. with-four way coupling, is very dependent on how ideal the collisions between the particles are. Ideal hard spheres, wood chips or gas bubbles react very differently to collisions, and the quality of the predicted viscosity will vary.

Granular flow models describe the rheology of a suspension of dry granular material. In the continuum framework, granular flow models are based upon simple models for particle interactions, and aim at transforming these interactions towards the continuum scale. Only a brief presentation of the models is given below, with no theoretical derivation of the equations. However, the presentation will give an understanding of what variables are important, e.g. the granular temperature, restitution coefficient and particle pressure.

There are three mechanisms for viscosity, namely particle movement, collision and friction, as shown in Figure 6.10. At low loading with large distances between the particles, most of the momentum transfer occurs by individual particles moving into areas with different average velocities before they collide and transfer momentum. This mechanism is similar to momentum transfer in gases. At higher loading, the particles can move only a short distance before they collide, and most of the momentum transfer

occurs by frequent collisions. This mechanism is similar to momentum transfer in liquids. In both these mechanisms, the viscosity depends on the fluctuation motion of the particles, i.e. the granular temperature defined below. At the highest loading the particles are in constant contact and slide over each other. Here the mechanism for momentum transfer is friction, and the viscosity depends on the granular temperature via the particle pressure p_{d}. Granular flow models are usually divided into two families of models, the slow granular flow models and the rapid granular flow models. Slow granular flow is related to momentum transfer by friction and frequent collision of particles in a dense environment, whereas in rapid granular flow the momentum transport occurs by movement and collision of particles.

A popular model in the rapid granular flow regime is the kinetic theory for granular flow [19]. The kinetic theory of granular flow predicts the stresses in moderately dense flows quite accurately, and it has successfully been employed in many applications in this regime. In the rapid granular flow regime, the solids stress arises from particle momentum exchange due to translation and collision. A key parameter in the constitutive closures for the solids phase is the energy associated with the fluctuating motion of the particles, the so-called granular temperature. The granular temperature is defined as the random movement of particles corresponding to how the random movement of molecules in kinetic theory of gases constitutes temperature,

$$\theta = \frac{1}{3}\left(\left\langle u_1^2\right\rangle + \left\langle u_2^2\right\rangle + \left\langle u_3^2\right\rangle\right), \tag{6.50}$$

where u represents the fluctuating velocity of a particle, which has a zero mean by definition. The kinetic theory of granular flows aims to derive a transport equation for the granular temperature. The shearing of the particles causes granular temperature to be produced, and the damping non-ideal component of the collisions, transferring kinetic energy to heat, causes a dissipative effect in granular temperature. The terms in the granular temperature balance arise from collisions and the streaming of particles. In this process, quite a few closures are required, and some of these remain topics for discussion and further research. The balance for granular temperature is very similar to the balance for thermal energy, Eq. (2.28) in Chapter 2. The equation is formulated as

$$\frac{3}{2}\left[\frac{\partial(\rho_{\mathrm{d}}\alpha_{\mathrm{d}}\theta)}{\partial t} + U_{j,\mathrm{d}}\frac{\partial(\rho_{\mathrm{d}}\alpha_{\mathrm{d}}\theta)}{\partial x_j}\right] = \kappa_{\mathrm{d}}\frac{\partial^2\theta}{\partial x_i\,\partial x_j} - p_{\mathrm{d}}\frac{\partial U_{j,\mathrm{d}}}{\partial x_j} + \tau_{kj,\mathrm{d}}\frac{\partial U_{k,\mathrm{d}}}{\partial x_j} - \gamma_{\mathrm{d}}, \tag{6.51}$$

where κ_{d} is the conductivity of granular temperature and the dissipation of fluctuation energy is described by

$$\gamma_{\mathrm{d}} = 3\left(1 - e_{\mathrm{d}}^2\right)\alpha_{\mathrm{d}}^2\rho_{\mathrm{d}}g_0\left(\frac{4}{d_{\mathrm{d}}}\sqrt{\frac{\theta}{\pi}} - \frac{\partial U_{i,\mathrm{d}}}{\partial x_i}\right), \tag{6.52}$$

where e_{d} is the coefficient of restitution for particle collisions. The models presented below are frequently used, but there is no general agreement on a best model. The granular temperature conductivity κ_{d} is a complex function of granular temperature,

restitution coefficient etc. that is not given here. The radial distribution function at particle contact is

$$g_0 = \left[1 - \left(\frac{\alpha_\mathrm{d}}{\alpha_{\mathrm{d,max}}}\right)^{1/3}\right]^{-1}, \tag{6.53}$$

where the maximum volume fraction of the dispersed phase $\alpha_{\mathrm{d,max}}$ is used to calculate a dimensionless particle–particle distance. This function (g_0) also certifies that the maximum particle loading is never surpassed by increasing the particle pressure to infinity when $\alpha_\mathrm{d} \to \alpha_{\mathrm{d,max}}$. The total particle pressure due to the streaming and collisions of particles is given as

$$p_\mathrm{d} = \alpha_\mathrm{d}\rho_\mathrm{d}\theta + 2\rho_\mathrm{d}(1+e_\mathrm{d})\alpha_\mathrm{d}^2 g_0\theta. \tag{6.54}$$

The kinetic and collision parts of the granular viscosity can be formulated as

$$\mu_{\mathrm{d,kin}} = \frac{\alpha_\mathrm{d} d_\mathrm{d}\rho_\mathrm{d}\sqrt{\theta\pi}}{6(1-e_\mathrm{d})}\left[1 + \frac{2}{5}(1+e_\mathrm{d})(3e_\mathrm{d}-1)\alpha_\mathrm{d} g_0\right], \tag{6.55}$$

$$\mu_{\mathrm{d,coll}} = \frac{4}{5}\alpha_\mathrm{d}\rho_\mathrm{d} d_\mathrm{d} g_0(1+e_\mathrm{d})\left(\frac{\theta}{\pi}\right)^{1/2}. \tag{6.56}$$

Slow granular flow models are based upon theories of soil mechanics, including a global inertia effect in the governing equations of the solids. The volume fractions of slow granular flows are typically very large, just below the maximum packing of the particles. Therefore, gradients of the volume fraction are typically neglected. The random kinetic energy of individual particles, the granular temperature, is very low and neglected as well. The granular flow is dominated by frictional stress, and the classical slow granular flow models based upon Mohr–Coulomb models have successfully been employed to predict the particle flow in, for instance, hoppers and chutes. Such models describe how normal pressure and viscosity depend upon the strain-rate tensor; for instance, for the frictional viscosity

$$\mu_{\mathrm{d,fr}} = \frac{p_\mathrm{d}\sin\phi}{2\sqrt{I_{2\mathrm{D}}}}, \tag{6.57}$$

where $I_{2\mathrm{D}}$ is related to the principal strain-rate tensor. Some parameters must be set in the model, i.e. the coefficient of restitution for particle collisions e_d and the angle of internal friction ϕ. The angle of internal friction ϕ is the maximum angle of a stable slope determined by friction, cohesion and the shapes of the particles.

Although rapid granular flow occurs less often in nature than slow granular flow, there are much sounder models for this flow regime. The basic assumption for such models is that particle interactions comprise binary, instantaneous and nearly elastic collisions. The particle rheology is directly expressed in the granular temperature. Since the number of particles is strongly dependent upon the solids volume fraction, the particle stresses have a strong dependence upon the solids volume fraction. When the solids volume fraction reaches the maximum packing, the number of collisions is infinite, and so are the predicted particulate stresses. Rapid granular flow models are not very accurate in this very dense regime, since the inter-particle interaction is no longer instantaneous,

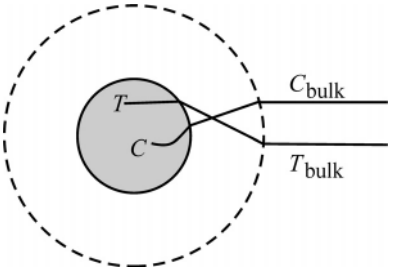

Figure 6.11 Mass and heat transfer between a particle and the bulk fluid.

and a transition to slow granular flow models should be made. For example, adding the stresses arising from the rapid granular flow regime to the slow granular flow regime,

$$\mu_{\text{d}} = \mu_{\text{d,kin}} + \mu_{\text{d,col}} + \mu_{\text{d,fr}}$$

gives a model that can handle the whole range of particle loading reasonably well.

6.4.3 Heat and mass transfer

Heat and/or mass transfer often plays an important role in multiphase flows. Examples are evaporating liquid droplets, reactions on catalysts, burning of coal particles and the creation of bubbles by means of cavitation. Models describing mass and heat transfer are typically quite crude and are built upon empirical or simplified relations of the Sherwood or Nusselt dimensionless parameters. The particles may be inert particles that can be heated or cooled, droplets that can evaporate or condense, fuel particles that may burn or catalyst particles that catalyse reactions.

When the net flow from or to the particle is small, mass transfer between a particle and the bulk fluid can be estimated using the film model. The mass flux [mol m^{-2} s^{-1}] is then expressed as

$$N_n = k_{\text{c},n}\left(C_{n,\text{s}} - C_{n,\text{bulk}}\right), \tag{6.58}$$

where $C_{n,\text{s}}$ is the concentration of species n on the surface and $C_{n,\text{bulk}}$ is the concentration in the fluid bulk surrounding the particle (Figure 6.11). The mass-transfer coefficient $k_{\text{c},i}$ is often described by a Sherwood number, Sh,

$$Sh = \frac{k_{\text{c},i} d_{\text{p}}}{D_i} = 2 + 0.6 Re_{\text{d}}^{1/2} Sc^{1/3}. \tag{6.59}$$

According to this correlation the mass transfer between particles and a fluid depends on the molecular diffusivity, the size of the particles, the viscosity and the relative velocity between the fluid and the particles. One advantage using CFD is that the local Re_{d} and local Sh are obtained. However, evaporation, condensation and chemical reactions cause a net flow to or from the particle that may decrease or increase mass and heat transfer, and Eq. (6.58) must be adjusted accordingly. The drag is also affected by the net flow to and from the particles.

Heat transfer is described in a similar way using the Nusselt number, Nu,

$$Nu = \frac{hd_\mathrm{p}}{\lambda} = 2 + 0.6Re_\mathrm{d}^{1/2}Pr^{1/3}, \tag{6.60}$$

and the heat balance of a particle is written

$$m_\mathrm{p}c_\mathrm{p}\frac{\mathrm{d}T_\mathrm{p}}{\mathrm{d}t} = hA_\mathrm{p}\left(T_\mathrm{bulk} - T_\mathrm{p}\right) + \frac{\mathrm{d}m_\mathrm{p}}{\mathrm{d}t}h_\mathrm{fg} + R\Delta H + A_\mathrm{p}\varepsilon_\mathrm{p}\sigma(T_\mathrm{surr}^4 - T_\mathrm{p}^4), \tag{6.61}$$

where m_p is the mass of the particle, h_fg the enthalpy of evaporation, R the reaction rate and ΔH the reaction enthalpy. In this balance we have included the accumulation of heat in the particle, the decrease in particle weight due to evaporation with corresponding heat loss, the heat due to a reaction in the particle and radiation from the particle to the surrounding.

In boiling, condensation and cavitation phase changes occur. This requires an additional term in the equation for conservation of mass,

$$\frac{\partial(\alpha_k\rho_k)}{\partial t} + \frac{\partial(\alpha_k\rho_k u_{i,k})}{\partial x_i} = \dot{m}_k, \tag{6.62}$$

where $\dot{m}_k$ represents the mass transfer from or to phase k per unit volume and unit time.

6.5 Boundaries and boundary conditions

When performing simulations with multiphase flows, boundary conditions should be given for each phase at each boundary. The boundary conditions for the continuous phase resemble the type of boundary condition for single-phase flows. At an inlet, a velocity profile or mass flow rate may be specified. Additionally, a volume fraction is often specified. If a turbulence model is employed for the continuous phase, the turbulence properties of the flow entering the domain should also be specified. At the outlet, typically a pressure or reference pressure is specified. If there is no backflow entering the outlet, the setting of most flow properties is not very important. If there is a flow entering the domain through the outlet, some of the outlet boundary conditions may be specified in a manner similar to what is done for an inlet.

At walls usually a 'no-slip' boundary condition is specified for the continuous phase, with additional wall functions when the flow is turbulent. Particle–wall collisions are of importance in most confined flows. Because particle–wall collisions are non-ideal, a particle–wall impact is associated with a deceleration of the particle, which is re-accelerated on re-entering the flow. Hence, a particle–wall impact indirectly extracts momentum from the continuous phase, causing a pressure loss. This effect is enhanced in the case of 'soft' walls.

6.5.1 Lagrangian dispersed phase

In Lagrangian particle simulations, particle–wall collisions are treated by using models similar to those for particle–particle collisions. If a hard-sphere model is adopted, the

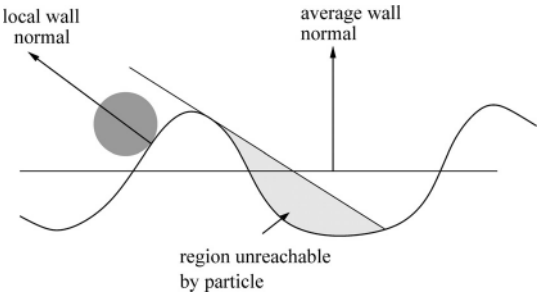

Figure 6.12 A particle colliding with a rough wall.

particle–wall collision may dissipate kinetic energy as heat that can be estimated from the coefficient of restitution. The restitution coefficient is defined as the ratio of the velocity after collision and that before collision. If a soft-sphere model is adopted, the effect of the wall may be described using a spring–slider–dashpot model based upon heuristics or upon a number of physical parameters. Note that, in the application both of hard-sphere and of soft-sphere models, the properties of the wall are not necessarily the same as the properties of the particles. Most often, a wall can be treated as a particle with infinite mass and radius.

Rough walls

Experiments and simulations have shown that wall roughness may have a considerable effect on the particle–wall collision process, and thus on the complete flow characteristics. This has two causes. First, the normal of the actual wall might not be constant across the wall. This means that the impact normal is a function of the local wall roughness. This can be modelled by including a 'random' component on top of the average wall normal. Secondly, the so-called shadow effect results in a shift of the effective roughness distribution for small impact angles. Both effects are shown in Figure 6.12: (1) the local wall normal changes along the wall, affecting the collision normal; and (2) particles with small impact angles can no longer collide with parts of the wall, making certain collision normals more likely than others (this was called the shadow effect by Sommerfeld in 1996).

6.5.2 Eulerian dispersed phase

Boundary conditions for walls in Eulerian models are less obvious than in the Lagrangian framework. In most simulations, particles are assumed to slip freely along the walls. This assumption originates from experimental observations, in which most particles seem to move rather freely along walls. More realistically, a slip condition can be specified at the walls,

$$\frac{\partial U_{i,\mathrm{d}}}{\partial n_i} = f, \tag{6.63}$$

where f specifies the amount of slip. If $f = 0$, the free-slip conditions are obtained. It is generally observed that convergence becomes difficult for higher values of f.

Boundary conditions for the granular temperature at the wall may have a significant impact on the flow. Various models that mimic the wall functions for single-phase turbulent flows are available. These have a production term, accounting for the dispersion effect of the particles, and a dissipation term, accounting for the non-ideal effect of the collision. In most simulations, specifying a zero gradient of granular temperature at walls gives satisfactory results.

6.6 Summary

In this chapter the Euler–Lagrange, Euler–Euler, mixture, volume-of-fluid and packed-bed models are presented. In many cases, it is not evident which model to choose. Each of the models is based on a number of assumptions and provides a specific level of detail. Some models describe individual particles or interface segments, whereas other models are expressed in terms of averaged properties. When selecting a model, numerical stability and computational cost must also be considered.

The *Euler–Euler* model is obtained by averaging the flow properties of a multiphase flow of dispersed particles smaller than the computational cells. The model solves the momentum and continuity equations for each phase. It is the most general model and should in principle work for all kinds of multiphase flows. However, it is usually less stable than the other models, and it requires closure models to describe all interactions between the phases, so empirical models for the specific system are often required. The *mixture* model is a simplification of the Euler–Euler model that is more stable but requires a strong coupling between the phases, i.e. low Stokes number. It shares with the Euler–Euler model the problem that empirical closures are required for any interaction between the phases.

In the *Euler–Lagrange* model the transport equations for each particle or a bundle of particles that behave identically are solved. It is most accurate and works very well for systems with a limited number of particles, often in cases in which particle–particle collisions can be neglected, i.e. when the particle–particle distance is larger than ten particle diameters. In principle, inter-particle collisions can be taken into account, but this is usually very expensive. The upper limit for the number of particles or bundles of particles is a few hundred thousand when the simulations are done on a PC. The model tracks the centre of gravity of the bundle, and a limit for the bundle size is that most of the particles in the bundle should be within one computational cell if one is to describe the interaction with the continuous phase accurately. The Euler–Lagrange model can easily take into account particle-size or density distributions. For a large size or density distribution the Euler–Euler model requires several phases to describe the system and relations to describe their interactions. In these cases, the Euler–Lagrange model will be more stable and will predict the flow better.

The *volume-of-fluid* (VOF) model is intended for gas–liquid and liquid–liquid segregated flows. The model resolves the interface between the phases and requires that the

Table 6.3 Suggested multiphase models for some common processes

System	Criterion	Example	Model
Gas/liquid–solid	Few particles or bundles of particles. Particle–particle distance $<10d_p$	Sedimentation	Euler–Lagrange
	Many particles $St < 1$	Stirred tank	Mixture
	Many particles $St > 1$	Fluidized bed Cyclone sedimentation	Euler–Euler
Bubbly flow	Few bubbles, bubble–bubble distance $>10d_p$		Euler–Lagrange
	Large volume fraction of gas	Bubble column	Mixture
Segregated gas–liquid	Large fluid particles	Slugs, waves	Volume of fluid
Sprays	Few drops or bundles of drops	Spray	Euler–Lagrange
Liquid–liquid	Stokes number $St < 1$	Extraction	Mixture
	Stokes number $St > 1$		Euler–Euler
	Large fluid particles		Volume of fluid
Gas–liquid–solid	Stokes number $St > 1$	Slurry reactor	Mixture
	Stokes number $St < 1$	Flotation	Euler–Euler

fluid particles, e.g. droplets or bubbles, are much larger than the computational cells. The phases are modelled using a single velocity field, and the computational cells that are shared between the phases have to be averaged. The model works well in flows with not too high a viscosity or density ratio between the phases. Since the method requires a DNS resolution of the flow at the interface, the damping of turbulence at the interface in turbulent flows is not well modelled and the VOF model may overestimate the shear stress at the interface. The model requires a large number of mesh cells, and Cartesian mesh cells make the method much more accurate.

The *porous-bed* model predicts flow in channels and cavities much smaller than the mesh. The model requires that the volume fraction of the continuous phase is given a priori and that the pressure drop is given by an algebraic model.

6.6.1 Guidelines for selecting a multiphase model

In selecting the best multiphase model, the first step is to identify the porous domains and attribute appropriate flow models to each area. The second step is to characterize the flow as segregated or dispersed. Other parameters that are important in selecting the best model are the particle loading and the Stokes number. The particle loading will give an estimate for the number of particles and the probability of particle–particle collisions. The Stokes number predicts how independently the dispersed phase behaves relative to the continuous phase. The scheme in Figure 6.13 gives a crude view of the choices. However, the choices are not clear-cut insofar as there might be other reasons for selection of models (Table 6.3). Very often it is the stability of the solution and available data that decide the selection.

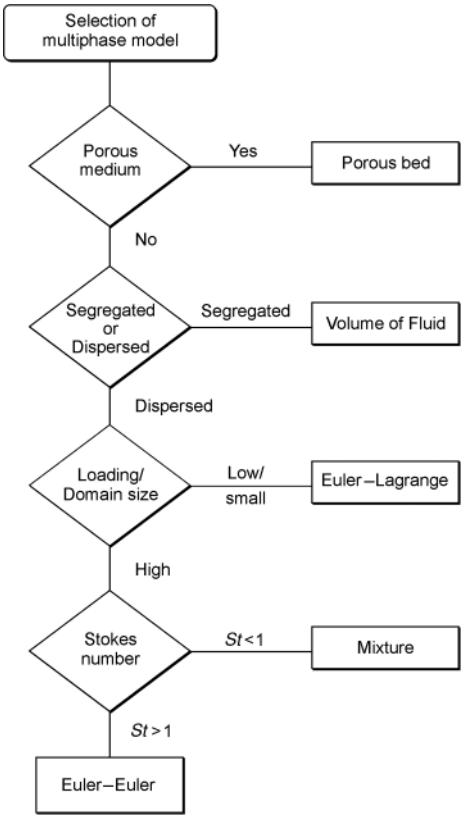

Figure 6.13 A schematic guide for the selection of multiphase models.

Questions

(1) Describe a few key parameters that are useful for characterizing multiphase flows.
(2) What is the physical interpretation of the Stokes number?
(3) Several forces act on a single particle in a fluid flow. Discuss the most important of these.
(4) Discuss what is meant by phase coupling.
(5) Explain what models it is appropriate to use for different types of dispersed phase flows and stratified flow.
(6) What closure models are required for multiphase flow simulations?
(7) Explain the concept of viscosity modelling for granular flows.